Strongly localized vectorial modes in nonlinear waveguide arrays

S. Darmanyan,[1,2] A. Kobyakov,[1] E. Schmidt,[3] and F. Lederer[1]
[1]*Institute of Solid State Physics and Theoretical Optics, Friedrich-Schiller-Universität Jena, Max-Wien-Platz 1, 07743 Jena, Germany*
[2]*Institute of Spectroscopy, Russian Academy of Sciences, Troitsk, Moscow region 142092, Russia*
[3]*Institute of Theoretical Physics, Friedrich-Schiller-Universität Jena, Max-Wien-Platz 1, 07743 Jena, Germany*
(Received 17 September 1997)

We report the existence of a variety of strongly localized bright vectorial modes in discrete cubic media with self- and cross-modulation. In addition to the modes familiar from the scalar limit, interesting types of solutions can be identified. These solutions are unique, to our knowledge, and have no analogs in other discrete or continuous models. The linear stability analysis of the vectorial modes discloses various instability scenarios, and permits us to draw conclusions for potential all-optical switching schemes. The analytical results obtained are confirmed by direct numerical simulations.
[S1063-651X(98)02903-1]

PACS number(s): 42.65.Wi, 42.81.Qb, 03.40.Kf

I. INTRODUCTION

It is now commonly believed that the remarkable peculiarities of nonlinear optical waveguide and fiber arrays can potentially be exploited in all-optical signal processing (signal steering and routing), amplification, and generation of pulse trains with a high repetition rate. The existence of intrinsically localized states in arrays with a cubic (Kerr) nonlinearity, where the field evolution can be described by the discrete nonlinear Schrödinger equation (DNLSE), has been proved, and their properties have been analyzed systematically [1–5]. As a consequence of these studies it was suggested to exploit localized states for power- and phase-controlled switching and steering [6–10]. Beyond the optical environment other nonlinear discrete systems, described by different equations, may exhibit bright and dark states that are almost entirely localized on a few sites (or even on a single site) [11–15]. Moreover, other phenomena such as modulational instability of plane waves, formation and stability of temporal solitons, and the recurrence effect occur in a quite different way compared to the continuum case (see Refs. [16–20], and references therein). Some theoretically predicted properties of discrete systems, e.g., the existence and dynamics of localized states, were experimentally verified [21,22].

As regards arrays of optical waveguides, the evolution of one-component fields, described by a single DNLSE, have been studied exclusively to date. However, a situation is frequently encountered where two waves, i.e., components with different frequencies or polarization states, copropagate in a waveguide. In this case the cubic nonlinearity provides a nonlinear coupling between these waves yielding to cross-phase modulation (XPM) and energy exchange. The latter effect can be neglected, provided that the wave-vector mismatch between both field components is large. In continuous systems the field dynamics can then be described by two incoherently coupled NLSE's, the properties and solutions of which were extensively studied (see Refs. [23,24], and the references therein). For the specific case of equal self-phase modulation (SPM) and XPM the system has proved to be integrable. An analytical expression for the resulting vector soliton could be derived by use of the inverse scattering transform [25]. However, the very effect of intrinsic localization in discrete systems with a two-component field, which can be described by two coupled DNLSE's (CDNLSE), has not been addressed to date.

The aim of this paper is to investigate strongly localized *vectorial* states of the CDNLSE systematically. We derive approximate analytical solutions for strongly localized modes (SLM's) of different topologies, study their stability by a linear analysis, and verify the results obtained by numerical experiments. It is shown that the topology of some vectorial localized states can considerably deviate from that of continuous vector solitons as well as from localized solutions in other discrete systems studied previously.

The paper is organized as follows: In Sec. II we introduce the CDNLSE under investigation, and discuss its parameters and normalization. In Sec. III, analytic expressions for vectorial bright SLM's of different topologies are derived. The stability analysis of typical SLM's is performed and implications for all-optical signal processing are discussed in Sec. IV.

II. BASIC EQUATIONS AND NORMALIZATION

In an array of n lossless, identical, and equidistant optical waveguide the propagation of the two-component envelope field can be described by a set of difference-differential equations as

$$i\frac{dE_n^{(1)}}{dZ}+C_1(E_{n+1}^{(1)}+E_{n-1}^{(1)})+(\lambda_{11}|E_n^{(1)}|^2+\lambda_{12}|E_n^{(2)}|^2)E_n^{(1)}=0,$$

$$i\frac{dE_n^{(2)}}{dZ}+C_2(E_{n+1}^{(2)}+E_{n-1}^{(2)})+(\lambda_{21}|E_n^{(1)}|^2+\lambda_{22}|E_n^{(2)}|^2)E_n^{(2)}=0. \quad (1)$$

Here $E_n^{(1)}$ and $E_n^{(2)}$ represent the field envelopes of both components in the nth channel, the evolution variable Z denotes

the spatial coordinate along the waveguide, and $C_{1,2}=\pi/(2L_{1,2})$ are the respective coupling coefficients, where $L_{1,2}$ are the half beat lengths of the corresponding two core coupler. The effective nonlinear coefficients $\lambda_{ij}=(\omega_i/2c)n_{ij}\rho_{ij}$ $(i,\ j=1,2)$ with $\rho_{ij}=\langle|R_i|^2|R_j|^2\rangle/\langle|R_i|^2\rangle$ include dimensionless functions R_i describing the transverse mode profile and the cubic nonlinear coefficients n_{ij}. The brackets denote integration over the cross section of the waveguide. For weakly guided modes in optical fibers, we have $\rho_{ij}\approx 0.5$ [23,24]. The transverse coupling in the array may be interpreted as ''discrete diffraction,'' which transforms to ordinary diffraction in the continuous limit.

Equations (1) can be recast in the more convenient Hamiltonian forms

$$i\frac{dA_n}{dz}+c_a(A_{n+1}+A_{n-1})+(\lambda_a|A_n|^2+|B_n|^2)A_n=0,$$

$$i\frac{dB_n}{dz}+c_b(B_{n+1}+B_{n-1})+(|A_n|^2+\lambda_b|B_n|^2)B_n=0, \quad (2)$$

where the scalings $c_{a,b}=C_{1,2}L_{\rm NL}$, $\lambda_a=\lambda_{11}/\lambda_{12}>0$, $\lambda_b=\lambda_{22}/\lambda_{12}>0$, $z=Z/|L_{\rm NL}|$, $A_n=\sqrt{|\lambda_{21}/\lambda_{12}|}(E_n^{(1)}/E_{\rm max}^{(2)})$, $B_n=E_n^{(2)}/E_{\rm max}^{(2)}$, and $L_{\rm NL}=(\lambda_{12}|E_{\rm max}^{(2)}|^2)^{-1}$ have been applied; $E_{\rm max}^{(2)}$ is the peak amplitude of the second field component.

As in the continuous model, system (2) describes coupling between modes which either oscillate at different frequencies ($\lambda_a\approx\lambda_b\approx 0.5$) or are orthogonally polarized in a highly birefringent waveguide. In the case of an elliptically birefringent fiber, $\lambda_a=\lambda_b$ varies between 0.5 and 1.5 depending on the angle of ellipticity [26].

Provided that the field envelopes vary slowly with n Eqs. (2) can be transformed into the extensively studied continuous system which describes pulse propagation in a dispersive medium with SPM and XPM. The existence of vectorial soliton solutions to this system gives some evidence that similar localized solutions may exist in the discrete case as well. However, the very existence of these discrete counterparts of the continuous solutions has not been reported to date. In this context it is worthwhile to study how the continuous solutions transform into discrete solutions of similar topology, and if there are solutions with new topologies which are formed owing to the discrete nature of the system.

III. BRIGHT SLM's OF THE CDNLSE

Highly localized solutions to Eq. (2) can be found by generalizing a method previously applied to one-dimensional nonlinear lattices [1,13] toward vectorial fields. We consider only resting solutions and can thus make the ansatz $A_n=\alpha_n\exp(ik_az)$ and $B_n=\beta_n\exp(ik_bz)$. The stationary amplitudes in each channel $\alpha_n=Aa_n$ and $\beta_n=Bb_n$ are normalized by the maximum values A and B, respectively. Without loss of generality these maximum amplitudes can attain either sign and are assumed to be real. Inserting A_n and B_n into Eq. (2) we arrive at a system of algebraic equations. Its solution yields the stationary excitations in each waveguide of an array (or equivalently on each site of a lattice) that eventually constitute SLM's of different topologies. We are now going to discuss these solutions in detail, where we attempt to introduce a systematic categorization with respect to the topology and the symmetry of the solutions. Furthermore we study how the variation of the array parameters (linear coupling, nonlinearity) as well as the input intensities of the two components (control parameter) affect the field evolution.

A. Odd SLM's

These modes are centered on site, and exhibit different symmetries. There are the conventional symmetric and antisymmetric solutions, but also new types that we term *shifted* modes. The latter represent vectorial modes where the maxima of the two components are located at different waveguides.

1. Symmetric mode

We insert $\alpha_n=A(\ldots,a_2,a_1,1,a_1,a_2,\ldots)$ and $\beta_n=B(\ldots,b_2,b_1,1,b_1,b_2,\ldots)$ into Eq. (2), and obtain, after straightforward calculations, the approximate analytic expression for this SLM as

$$k_a=\lambda_aA^2+B^2, \quad k_b=A^2+\lambda_bB^2 \quad (3)$$

for the corresponding wave vectors, and

$$a_1\equiv a\approx c_a/k_a\ll 1, \quad b_1\equiv b\approx c_b/k_b\ll 1 \quad (4)$$

for the secondary excitations. This approximation is consistent with the very subject of our studies, namely, *strongly* localized modes. Note that the peak amplitudes A and B are arbitrary parameters. We can calculate the secondary excitations with any desired accuracy. But because we are primarily interested in physical aspects of the problem, we restrict ourselves to the first-order approximation with respect to the small parameters $a,b\ll 1$,and neglect $a_2\propto a^2$ and $b_2\propto b^2$ together with the higher-order terms. As will be shown below, these first-order calculations usually provide a sufficient accuracy to understand the basic SLM properties. But, if required, we take into account higher-order terms in conjunction with excitations of adjacent channels.

It is worth mentioning that the solutions found exist both for positive (focusing) and negative (defocusing) nonlinearity λ_{ij}. According to the normalization, the latter reverses the sign of the normalized coupling constant $c_{a,b}\rightarrow -c_{a,b}$, which implies a phase shift π between subsequent sites. Thus, assuming a positive coupling $C_{1,2}$, which is physically meaningful only, and defocusing nonlinearity ($\lambda_{ij}<0$), we obtain the so-called *staggered* SLM's [5]. These modes are characterized by a π phase change from channel to channel. To illustrate the structure of the different modes, they are schematically drawn in Fig. 1.

2. Antisymmetric mode

Antisymmetric modes represent another family of solutions, and are characterized by a zero amplitude at the central site. Analogously to the previous case, this type of mode can be found by use of the approximate ansatz $\alpha_n\approx A(\ldots,0,0,a,1,0,s_a,s_aa,0,0,\ldots)$ and $\beta_n\approx B(\ldots,0,0,b,1,0,s_b,s_bb,0,0,\ldots)$, where s_a and s_b are scaling factors. They include the possible change of the phase by π across the mode. Substitution of α_n and β_n into Eq. (2) immediately yields $s_a=s_b=-1$, revealing the antisymmetric character of the solution with respect to the central site with

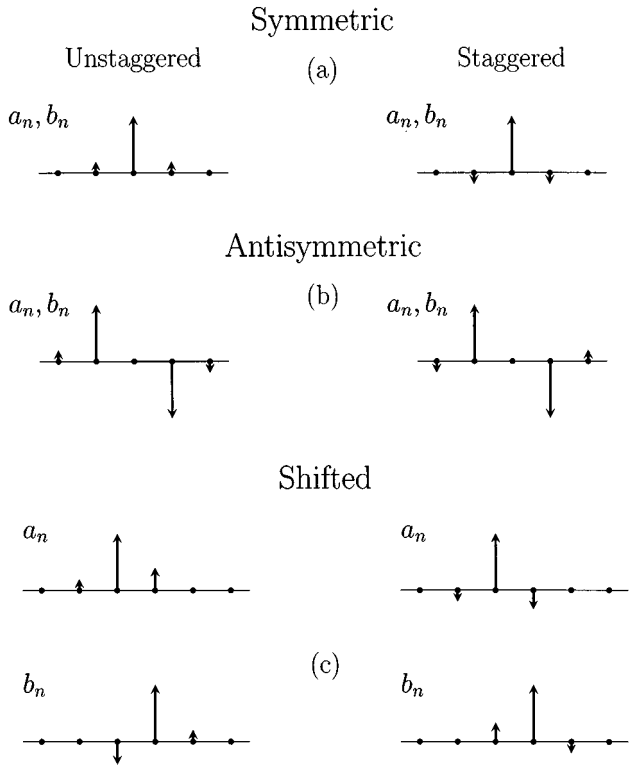

FIG. 1. Schematic representation of different kinds of odd modes. Unidirectional and contradirectional arrows denote in-phase and out-of-phase (π phase shift) oscillations of the electric field. Right- and left-hand side charts show staggered (defocusing nonlinearity $\lambda_{ij}<0$,) and unstaggered (focusing nonlinearity $\lambda_{ij}>0$) SLM's, respectively.

zero amplitude [Fig. 1(b)]. The wave vectors and secondary excitations of this SLM coincide with those given by Eqs. (3) and (4). Note that this type of mode can be viewed as a superposition of two symmetric odd SLM's with a phase difference π. The zero amplitude at the central site results from opposite signs and equal amplitudes of the secondary excitations there.

3. Shifted odd mode

The substitution $\alpha_n \approx A(\ldots,0,a_{-1},a_0=1,a_1,0,0,\ldots)$ and $\beta_n \approx B(\ldots,0,0,b_0,b_1=1,b_2,0,\ldots)$ into Eq. (2) reveals another family of bright odd SLM's [Fig. 1(c)]. The secondary excitations of this mode,

$$a_{-1}=c_a/(\lambda_a A^2), \quad a_1=c_a/(\lambda_a A^2-B^2),$$

$$b_0=c_b/(\lambda_b B^2-A^2), \quad b_2=c_b/(\lambda_b B^2), \tag{5}$$

can again be derived from the corresponding set of algebraic equations. The existence of such a SLM is a consequence of the vectorial character of interaction. The corresponding fields a_n and b_n may have an asymmetric structure [Fig. 1(c)].

Note that expressions (5) are only valid for strongly localized modes, i.e., for $|a_{-1,1}| \ll 1$ and $|b_{0,2}| \ll 1$. Hence the evolution of this mode is drastically affected by the ratio of the peak amplitudes A/B. In Fig. 2 the evolution of the field intensities $|b_0|^2$ and $|b_1|^2$ in two adjacent channels ($n=1$ [Fig. 2(a)] and $n=0$ [Fig. 2(b)]) is shown as a function of the amplitude $\alpha_0=A$. Equal coupling and nonlinear coefficients for both components have been assumed. Evidently, the shifted mode is formed and propagates stable if $|A^2-B^2|$ exceeds some critical value. Otherwise, the mode is unstable, i.e., there is a periodic energy exchange between channels $n=0$ and $n=1$.

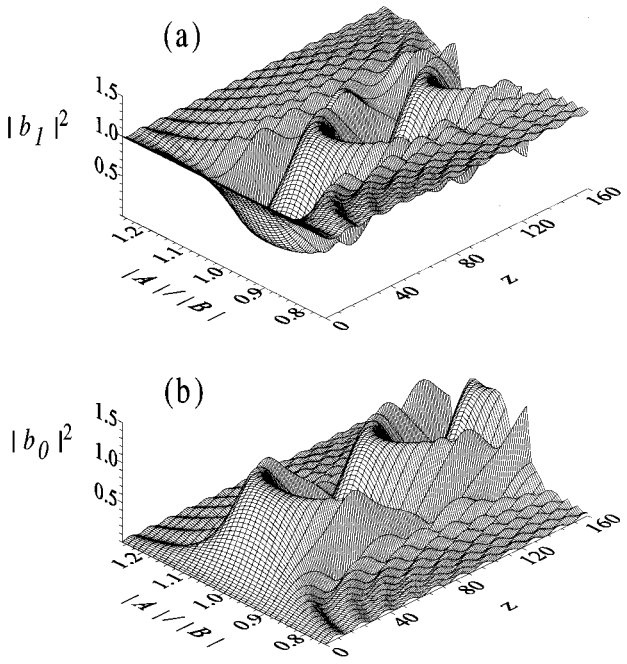

FIG. 2. Intensity of the B component in the two adjacent channels $n=1$ (a) and $n=0$ (b) as a function of the ratio of peak amplitudes $|A|/|B|$ and the propagation distance z. All quantities used in this and in the following figures are dimensionless. Parameters: $c_a=c_b=0.2$, $\lambda_a=\lambda_b=1$, and $B=1$.

B. Even SLM's

Now we proceed with even SLM's which are centered between the array sites. There is a greater diversity of solutions compared to the previous situation, because in this case more waveguides are involved (for a systematic overview, see Fig. 3).

Bright even symmetric SLM's can be classified as unstaggered ($c_{a,b}>0$) and staggered ($c_{a,b}<0$) depending on whether the excitations in adjacent waveguides are in phase or out of phase, respectively [Fig. 3(a)]. Moreover, like the scalar DNLSE, the CDNLSE admits a family of even SLM's which are characterized by a phase jump π at the center, and can thus be termed *twisted* modes [Fig. 3(b)]. We will show below that the stability behavior of these modes differs qualitatively from that of odd staggered and unstaggered SLM's.

Furthermore the coupled system (2) provides a new family of even solutions, namely, asymmetric SLM's [Figs. 3(c) and 3(d)]. These modes have no counterparts in continuous or in other discrete models. Finally, there is also a family of shifted even solutions [Fig. 3(e)].

1. Symmetric modes

We start with the class of symmetric SLM's of the forms $\alpha_n \approx A(\ldots,0,0,a,1,s_a,s_a a,0,0,\ldots)$ and β_n

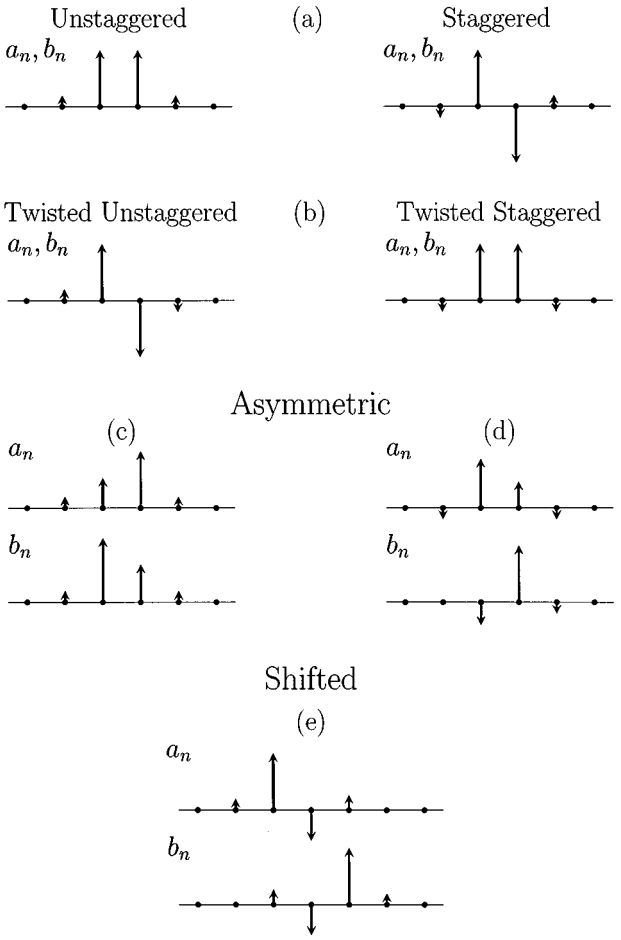

FIG. 3. Same as in Fig. 1 for even modes.

$\approx B(\ldots,0,0,b,1,s_b,s_b b,0,0,\ldots)$, where for the symmetric case Eq. (2) requires $s_{a,b}=\pm 1$ to hold. Thus the corresponding wave vectors and amplitudes of the secondary excitations are given in a first-order approximation by

$$k_a = c_a s_a + \lambda_a A^2 + B^2, \quad k_b = c_b s_b + A^2 + \lambda_b B^2 \tag{6}$$

$$a = c_a / k_a, \quad b = c_b / k_b. \tag{7}$$

Owing to $|a|,|b \ll 1$ the modes are again strongly localized. Similarly to the respective odd modes, the wave vectors and the secondary amplitudes are not affected by the sign of A and B (i.e., phase 0 or π for the entire solution). Recalling that for a defocusing nonlinearity ($\lambda_{ij}<0$) the coupling coefficients are negative, it follows from Eq. (7) that $a,b<0$. Now it is clear that four different types of symmetric modes can exist. For $a,b>0$ we obtain *unstaggered* modes [Fig. 3(a), left] being antisymmetric or *twisted* for $s_{a,b}=-1$ [Fig. 3(b), left]. Conversely, staggered modes appear for $a,b<0$ [Fig. 3(a), right], and twisted modes here require $s_{a,b}=1$ to hold [Fig. 3(b), right]. Note that a symbiotic pair of (un)staggered and twisted (un)staggered components is also possible.

2. Asymmetric modes

These modes can be obtained upon substitution of the asymmetric ansatz $\alpha_n \approx A(\ldots,0,0,a_{-2},a_{-1}=1,a_1=s_a,s_a a_2,0,0,\ldots)$ and $\beta_n \approx B(\ldots,0,0,s_b b_{-2},b_{-1}=s_b,b_1=1,b_2,0,0,\ldots)$ into Eq. (2), where the subscript $n=0$ has been dropped for convenience. Here $|s_{a,b}|<1$, which complicates the analysis considerably. From the corresponding set of algebraic equations we obtain the wave vectors and the secondary amplitudes

$$k_a = c_a s_a + \lambda_a A^2 + s_b^2 B^2, \quad k_b = c_b s_b + s_a^2 A^2 + \lambda_b B^2, \tag{8}$$

$$a_2 = a_{-2} = c_a / k_a, \quad b_2 = b_{-2} = c_b / k_b. \tag{9}$$

The amplitudes s_a and s_b that enter Eqs. (8) and (9) are determined by

$$(c_a - \lambda_a A^2 s_a)(s_a^2 - 1) + B^2 s_a (s_b^2 - 1) = 0,$$

$$(c_b - \lambda_b B^2 s_b)(s_b^2 - 1) + A^2 s_b (s_a^2 - 1) = 0. \tag{10}$$

Analytical solutions to Eq. (10) can be found only in some particular cases. For example, assuming $s_a = s_b$, one immediately obtains this value together with a condition for the ratio of the peak amplitudes

$$s_a = s_b = \frac{c_a + c_b \lambda_a}{B^2(\lambda_a \lambda_b - 1)}, \quad A^2/B^2 = (c_a \lambda_b + c_b)/(c_b \lambda_a + c_a). \tag{11}$$

As can be easily seen from Eq. (11), these solutions do not exist for $\lambda_a \lambda_b \approx 1$. One of the possible realizations of this mode is shown schematically in Fig. 3(c).

Another case which is analytically solvable requires that one of the excitations s_a or s_b is much less than unity. For $|s_b| \ll 1$ and $|s_a| \cong 1$, the approximate solutions to Eq. (10) can be written as

$$s_a^2 \approx 1 - \frac{B^2}{\lambda_a A^2}\left(1 + \frac{c_a}{\sqrt{(\lambda_a A^2)^2 - \lambda_a (AB)^2}}\right),$$

$$s_b \approx \frac{c_b \lambda_a}{B^2(\lambda_a \lambda_b - 1)} \ll 1. \tag{12}$$

This particular of a SLM can be viewed as a bound state formed by an even asymmetric mode (A_n) and an odd mode (B_n) [Fig. 3(d)].

3. Shifted even mode

To obtain this mode we write $\alpha_n \approx A(\ldots,0,a_{-2},a_{-1}=1,a_1,a_2,0,0,\ldots)$ and $\beta_n \approx B(\ldots,0,0,b_{-1},b_1,b_2=1,b_3,0,\ldots)$ to obtain

$$k_a = \lambda_a A^2 + c_a a_1, \quad k_b = \lambda_b B^2 + c_b b_1,$$

$$a_{-2} = c_a / k_a, \quad a_2 = c_a a_1 / (k_a - B^2), \quad b_3 = c_b / k_b,$$

$$b_{-1} = c_b b_1 / (k_b - A^2), \tag{13}$$

where the amplitudes of the excitations a_1 and b_1 are the solutions of

$$(c_a - \lambda_a A^2 a_1)(1 - a_1^2) + B^2 b_1^2 a_1 = 0,$$

$$(c_b - \lambda_b B^2 b_1)(1 - b_1^2) + A^2 a_1^2 b_1 = 0. \tag{14}$$

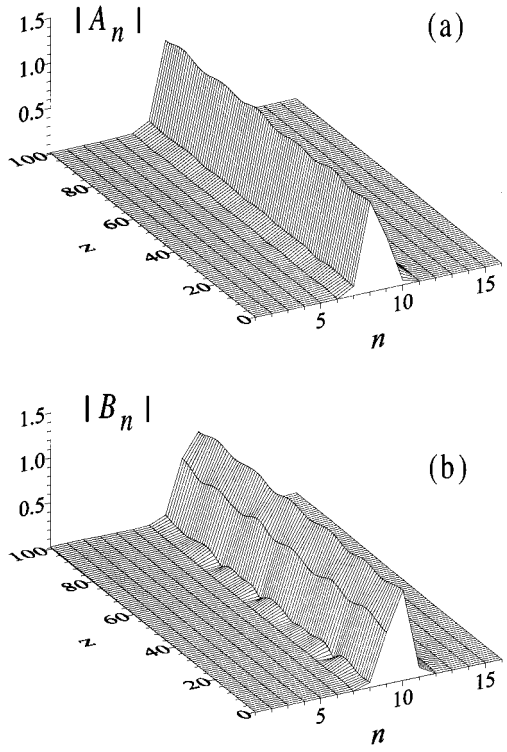

FIG. 4. Stable propagation of a perturbed even-shifted SLM schematically shown in Fig. 3(e). Parameters: $c_a=c_b=0.05$, $\lambda_a=\lambda_b=0.5$, and $A=B=1$. The waveguides are labeled by positive numbers.

For relatively large amplitudes $a_1 \gg c_a/(\lambda_a A^2)$ and $b_1 \gg c_b/(\lambda_b B^2)$, Eq. (14) exhibits approximate solutions

$$a_1^2 \approx \frac{\lambda_b(\lambda_a A^2 - B^2)}{A^2(\lambda_a\lambda_b - 1)}, \quad b_1^2 \approx \frac{\lambda_a(\lambda_b B^2 - A^2)}{B^2(\lambda_a\lambda_b - 1)}. \tag{15}$$

A numerical experiment proves (see Fig. 4) that this shifted mode may propagate stable even if the initial profile is calculated by using the approximate formula (15). Here equal peak amplitude $A=B$ have been used. The peculiarity of this mode is worth noting, viz., only one excitation of each component, i.e., a_1 and b_1, exhibits the π phase shift [Fig. 3(e)]. This distinguishes this SLM from the unstaggered as well as the twisted modes.

Another solution to Eq. (14) can be obtained in the limiting case of very small excitations, $|a_1|,|b_1| \ll 1$. Then $a_1 \approx c_a/(\lambda_a A^2)$ and $b_1 \approx c_b/(\lambda_b B^2)$, and the shifted even mode transforms into the doubly shifted odd mode.

IV. STABILITY ANALYSIS OF BRIGHT SLM's

In Sec. III, the existence of various stationary vectorial solutions of the CNLDSE, that are strongly localized across the array, was shown. Obviously, the stability of these SLM's is an important issue which will now be addressed. This subject is of particular interest here for two reasons. First, because the solutions were derived by using some approximation, they contain some ''intrinsic perturbation.'' Thus the question arises immediately if these modes transform adiabatically into stable, stationary solutions of the complete CNLDSE (2). Second, implications for all-optical switching and beam steering can be derived in identifying the boundaries in parameter space between stable and unstable domains.

In the literature, various approaches were used to investigate the stability behavior of strongly localized solutions in discrete systems. Obviously, a complete scan of the parameter space is inappropriate by means of a direct numerical integration of Eq. (2). Another evaluation of the stability relies on the so-called Peierls-Nabarro (PN) barrier [4,5]. According to this concept, odd and even modes of the same topology can be considered as two realizations of a common mode centered either on-site or between the sites. Now for odd and even SLM's of equal intensities, the difference in the corresponding Hamiltonians (viz. the PN barrier) determines which of the two realizations corresponds to the minimum energy and hence is stable. To interpret the results correctly, a negative effective mass has to be introduced for staggered solutions [5]. Being only a qualitative method, the PN approach provides no information about the instability gain, and fails in analyzing the stability of twisted modes because they lack an odd counterpart. Eventually, the variational approach was applied to study the stability of relatively weakly localized modes of the generalized DNLSE [27], and the chaotic behavior of solutions of three coupled NLSE's was predicted by calculating the Lyapunov exponent [28,29].

A clear and instructive alternative to tackle the stability problem consists of performing a direct linear analysis. Using this approach, it was shown [30] that, in contrast to the DNLSE, the odd localized modes of the Fermi-Pasta-Ulam lattice are unstable, whereas even modes have been proven to be stable. Although this method cannot predict the ultimate evolution of an unstable SLM, it accurately describes the onset of instability and yields the initial instability gain, i.e., the decay rate of the mode.

To investigate the stability, we impose complex perturbations $\varepsilon_n(t)$ and $\delta_n(t)$ on each nonzero excitation of both components of the vectorial SLM's. Beginning with even modes, we insert the perturbed stationary solutions $\alpha_n = A(\ldots 0,0,a+\varepsilon_{-2},1+\varepsilon_{-1},s_a+\varepsilon_{+1},s_a a+\varepsilon_{+2},0,0,\ldots)$ and $\beta_n = B(\ldots 0,0,b+\delta_{-2},1+\delta_{-1},s_b+\delta_{+1},s_b b+\delta_{+2},0;0,\ldots)$ into the governing equations (2). Neglecting all nonlinear terms in the small parameters $a,b,\varepsilon_{\pm j}$, and $\delta_{\pm j}(j=1,2)$, we obtain a set of eight coupled complex ordinary differential equations that is equivalent to a 16th-order eigenvalue problem. But, the analysis can be simplified considerably by using a proper decomposition of the perturbations $\varepsilon_j^{\pm} = \varepsilon_{+j} \pm \varepsilon_{-j}$ and $\delta_j^{\pm} = \delta_{+j} \pm \delta_{-j}$ into symmetric $(+)$ and antisymmetric $(-)$ components. In doing so, the dimension can be reduced by a factor of 2 because the problem splits into two independent parts. After the separation of real and imaginary parts of the perturbations $\varepsilon_j^{\pm} = \varepsilon_{jr}^{\pm} \pm i\varepsilon_{ji}^{\pm}$ and $\delta_j^{\pm} = \delta_{jr}^{\pm} \pm i\delta_{ji}^{\pm}$, we arrive at the eighth-order eigenvalue problem for real variables:

$$\frac{d\mathbf{P}}{dz} = \begin{pmatrix} \mathbf{M}_A & \tilde{\mathbf{M}}_A \\ \mathbf{M}_B & \mathbf{M}_B \end{pmatrix} P. \tag{16}$$

Here the perturbation vector $\mathbf{P}^{\pm,\pm}$

$=(\varepsilon_{1r}^{\pm},\varepsilon_{1i}^{\pm},\varepsilon_{2r}^{\pm},\varepsilon_{2i}^{\pm},\delta_{1r}^{\pm},\delta_{1i}^{\pm},\delta_{2r}^{\pm},\delta_{2i}^{\pm})^T$ contains either symmetric $(+,+)$ or antisymmetric $(-,-)$ perturbations of both fields if the components of the vectorial SLM exhibit the same symmetry ($s_a=s_b$). For $s_a=-s_b$, symmetric perturbations $(+)$ of one component are coupled to antisymmetric ones $(-)$ of the other component, i.e., $\mathbf{P}^{\pm,\mp}=(\varepsilon_{1r}^{\pm},\varepsilon_{1i}^{\pm},\varepsilon_{2r}^{\mp},\varepsilon_{2i}^{\mp},\delta_{1r}^{\mp},\delta_{1i}^{\mp},\delta_{2r}^{\mp},\delta_{2i}^{\mp})^T$. The square 4×4 submatrices $M_{A,B}$ and $M_{A,B}$ have the forms

$$\mathbf{M}_A=\begin{pmatrix} 0 & c_a(p-s_a) & 0 & c_a \\ -2\lambda_a A^2-c_a(p-s_a) & 0 & -c_a & 0 \\ 0 & c_a & 0 & -(c_a s_a+\lambda_a A^2+B^2) \\ -c_a & 0 & c_a s_a+\lambda_a A^2+B^2 & 0 \end{pmatrix},$$

$$\mathbf{M}_B=\begin{pmatrix} 0 & c_b s_b(s_a p-1) & 0 & c_b \\ -2\lambda_b B^2-c_b s_b(s_a p-1) & 0 & -c_b & 0 \\ 0 & c_b & 0 & -(c_b s_b+A^2+\lambda_b B^2) \\ -c_b & 0 & c_b s_b+A^2+\lambda_b B^2 & 0 \end{pmatrix}, \tag{17}$$

where p denotes the symmetry of the perturbation, i.e., $p=1$ and -1 correspond to the upper and lower sign in the expression for the perturbation vector, respectively. Both submatrices $\tilde{\mathbf{M}}_{A,B}=\tilde{q}_{kl}^{A,B}$ have only one nonzero element, viz. $\tilde{q}_{21}^{A}=-2s_a s_b B^2$ and $\tilde{q}_{21}^{B}=-2s_a s_b A^2$, respectively.

Scalar limit. Before proceeding with the stability analysis of the vectorial modes, we concisely review the scalar case for the sake of comparison. If either B or A vanishes, Eq. (16) simplifies to the eigenvalue problem of the scalar case which was studied in detail in Ref. [31]. If we introduce $\varepsilon^{\pm}\propto\exp(Gz)$, where for an even scalar mode $k=k_a|_{B=0}$ is given by Eq. (6), the scaled eigenvalues $g=G/k$ can be derived from the biquadratic equation

$$g^4+[1+2(p-s)a+2(3-2ps)a^2]g^2 +2(p-s)a+2(3-2ps)a^2=0, \tag{18}$$

where $s_a=s$. If the symmetry of the perturbation coincides with that of the SLM ($s=p$), Eq. (18) does not exhibit real-valued solutions provided that a is small as required. Thus the SLM is always stable against those perturbations. This result has been verified numerically. Conversely, if the perturbation has the opposite symmetry of the SLM ($p=-s$) the SLM can become unstable [$\mathrm{Re}(g)\neq0$]. We observed two basically different kinds of SLMs dynamics. Both staggered and unstaggered modes ($sa>0$) are always unstable with respect to symmetric and antisymmetric perturbations, respectively, and the gain of instability

$$g\approx2\sqrt{sa}(1-5sa/4) \tag{19}$$

increases with a (see Fig. 5, upper branches). In agreement with the previously reported results [4,5,27], the instability of unstaggered modes is confirmed by a direct numerical solution of the DNLSE. The perturbed unstaggered (staggered) SLM decays and transforms subsequently into an odd mode. For relatively small amplitudes ($a\approx0.1$) the intermediate asymmetric, oscillating state is fairly persistent, and can be thus considered a quasistationary state.

In contrast to (un)staggered SLM's, modes with $sa<0$, namely, *twisted staggered* (TS) ($s=1$, $a<0$) and *twisted unstaggered* (TU) ($s=-1$, $a>0$) SLM's, are unstable only if the modulus of the amplitude a exceeds some critical value, i.e., $|a|>a_{\mathrm{cr}}\approx0.12$. The corresponding gain is

$$g\approx\sqrt{(-sa-a_{\mathrm{cr}})/2},\quad sa+a_{\mathrm{cr}}<0 \tag{20}$$

(see Fig. 5, lower curves). The stability of the twisted modes can be explained by the fact that neither the TU nor TS mode has a topological counterpart among odd SLM's. Hence such a twisted SLM cannot transform into an odd one, and stability arguments based on the PN barrier do not apply here. Beyond the critical value a_{cr}, the onset of instability manifests itself in a spreading of the mode, and sets in if the localization becomes weaker because of an increasing secondary amplitude $|a|$. Note that the instability regions as well as the gain do not significantly change if second-order terms and excitations at sites $|n|=3$ are taken into account.

Coming back to the vectorial case, one can show that the corresponding eigenvalue problem (16) can be reduced to a quartic algebraic equation for the squared eigenvalues μ, where a positive real part of $g=\pm\sqrt{\mu}$ represents the instability gain [$P\propto\exp(Gz)$, $G=gk_a$]. If both components of the

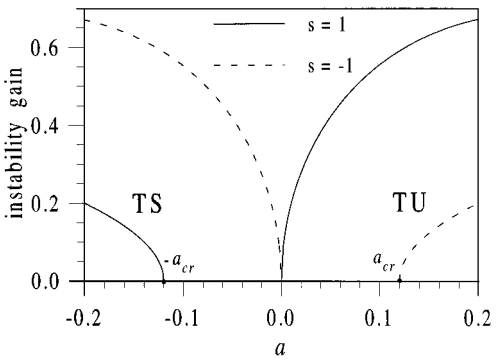

FIG. 5. Instability gain as a function of the secondary amplitude a for even SLM's in the limit of the scalar DNLSE. Upper curves apply to (un)staggered modes, and lower curves to twisted SLM's.

SLM have the same symmetry ($s_a = s_b = s$), equal peak amplitudes ($A = B$), and linear ($c_a = c_b = c$) and nonlinear coupling ($\lambda_a = \lambda_b = \lambda$), the characteristic polynomial of Eq. (16) can be factorized into four easily solvable biquadratic equations. We will show below that basic tendencies of SLM's evolution can be derived from this particular case. Hence we initially focus on these conditions which are also quite realistic.

The essential results compare to those obtained for the scalar DNLSE. However, the vectorial nature of the interaction introduces some new effects even if both components of the SLM are equal. As expected, both unstaggered and staggered even modes ($sa > 0$) are always unstable: the former with respect to the antisymmetric ($p = -1$) perturbation and the latter with respect to the symmetric ($p = 1$) one. In both cases the instability gain coincides with that in the scalar case (19) and, in addition, another eigenvalue of (16) evokes the nonvanishing instability gain

$$g \approx 2\left(\frac{\lambda - 1}{\lambda + 1}\, sa\right)^{1/2} \tag{21}$$

if $\lambda > 1$. The decay character of the respective SLM's resembles that encountered in the scalar situation. The antisymmetrically perturbed unstaggered SLM transforms into the odd mode in both components, as illustrated in Fig. 6(a). However, being qualitatively the same, the transformation of the even mode may result in an asymmetric odd state with different peak amplitudes [Fig. 6(a)]. The transition distance to the resulting odd state depends drastically on the value of the secondary amplitude. If the secondary amplitude decreases, the intermediate oscillating state [Fig. 6(a)] becomes fairly persistent, and the small satellite pulse decouples only after the localized structure adiabatically loses some energy due to diffraction across the array. There is no strong dependence on the sign of nonlinearity, and practically the same evolution was observed for $\lambda < 1$ as well. Here only the gain given by Eq. (19) causes the decay. This behavior can be anticipated because the odd mode is the only stable counterpart of the even unstaggered SLM. The asymmetric state the system passes through is unstable, while another potential state to transfer to, the stable shifted odd mode, does not exist for equal peak amplitudes A and B.

The evolution of the SLM appears differently if both components of the mode are antisymmetrically perturbed [Fig. 6(b)]. These initial conditions provoke a nonstationary oscillatory solution. Note that an intense anharmonic energy exchange between the two waveguides [Fig. 6(b)] occurs only if the nonlinearity exceeds some critical value $\lambda > \lambda_{cr}$, whereas for $\lambda < \lambda_{cr}$ both components exhibit periodic oscillations whose amplitudes do not exceed the amplitude of the perturbation. The critical value of the nonlinearity where the systems undergoes bifurcation depends on the array parameters and amounts to $\lambda_{cr} \approx 1.4$ for the situation depicted in Fig. 6. We stress, however, that any asymmetric perturbation causes a fast decay of the solutions reminiscent to that shown in Fig. 6(a).

If both the perturbation and the mode exhibit the same symmetry ($s_{a,b} = p$), a positive eigenvalue of Eq. (16) indicates a small nonzero gain $G = gk_a \approx |c|\sqrt{2(1-\lambda)/(1+\lambda)}$ for $\lambda < 1$. This gain is quite different from that described above, viz. it is linearly proportional to the coupling constant c and, more important, independent of the peak amplitude A. To check whether this behavior originates from the lack of accuracy introduced by the first-order approximation, we took second-order terms into account in the small parameter a, as well as the next-order excitations ($n = \pm 3$) which are likewise of the order of a^2. The respective calculations again result in a positive eigenvalue, but are already proportional to c^2. This clearly shows the artificial character of this instability gain. This result was confirmed by numerical studies. We also mention that in accounting for higher-order terms the genuine gain given by Eqs. (19) and (21) is only slightly modified. Therefore, even unstaggered (staggered) modes are stable with respect to symmetric (antisymmetric) perturbation.

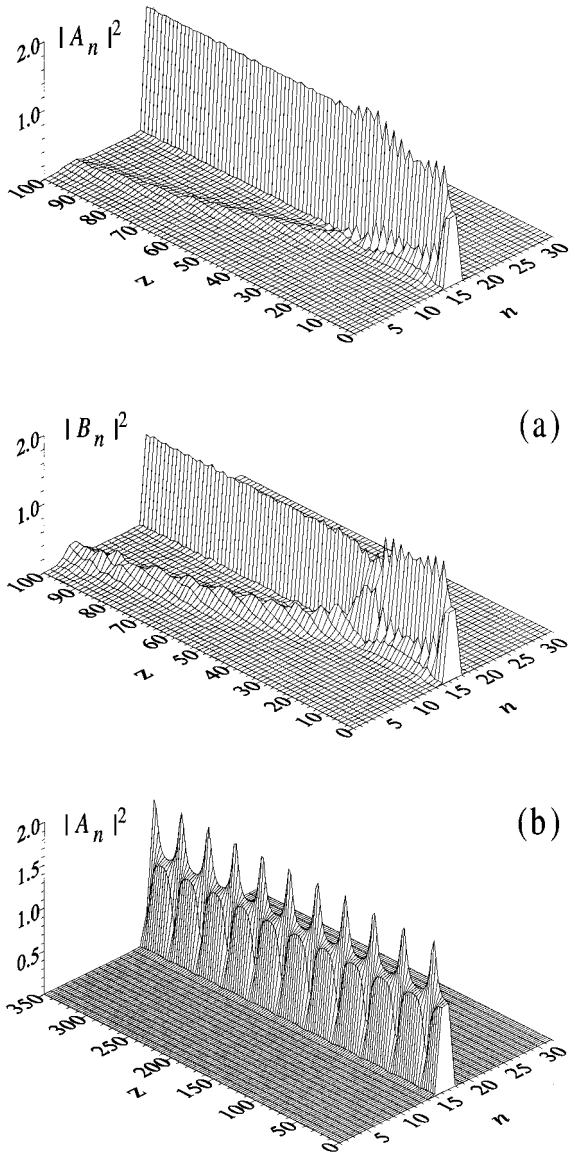

FIG. 6. Evolution of a perturbed symmetric unstaggered vectorial SLM ($s_a = s_b = s = 1$). Parameters: $\lambda_a = \lambda_b = \lambda = 1.5$, $A = B = 1$, and $c_a = c_b = c = 0.44$. (a) $\mathbf{P}^{-,-} = (0.01,0,0,0,0,0,0,0,0,0)$ is the transition to the odd mode, (b) $\mathbf{P}^{-,-} = (0.01,0,0,0,0, -0.01,0,0,0,0)$; the B component has the same oscillatory behavior.

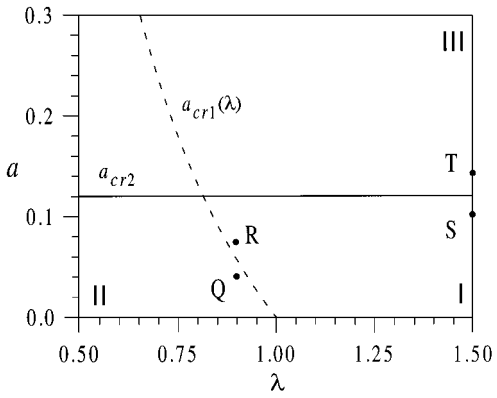

FIG. 7. Analytically calculated regions of stability and instability of twisted vectorial SLM's with equal peak amplitudes $A=B$. (I) Stable propagation of the mode. (II) Instability due to real positive eigenvalues. (III) Instability due to complex eigenvalues.

This behavior of even symmetric SLM's may find applications in digital information processing. Small perturbations of one component launched into waveguides $n=1(\varepsilon_1)$ and $n=-1(\varepsilon_{-1})$ serve as signals. If both signals are input simultaneously ($\varepsilon_1=\varepsilon$ and $\varepsilon_{-1}=\varepsilon$, which denotes a logic 1 in both channels) or in the absence of any perturbation ($\varepsilon_1=0$ and $\varepsilon_{-1}=0$, logic zero) the output intensity in both channels is high because the mode is stable with respect to the symmetric perturbation. Conversely, if only one signal ε_1 (ε_{-1}) is launched, the output intensity of *both components* in the channel $n=1$ ($n=-1$) is high, whereas the intensity in the adjacent channels is almost zero [Fig. 6(a)]. Thus the logic function $\varepsilon_1+\overline{\varepsilon}_{-1}$ (the bar denotes logic negation) in channel $n=1$ and the complementary function $\overline{\varepsilon}_1+\varepsilon_{-1}$ in channel $n=-1$ can be realized.

Unlike the (anti)symmetrically perturbed (un)staggered modes that always transform to an odd mode, the perturbed twisted modes may exhibit three different types of evolution depending on the nonlinearity and the degree of localization (Fig. 7). The linear analysis predicts stable upper bound set by the critical secondary amplitudes a_{cr1} and a_{cr2}, respectively, as

$$|a_{\mathrm{cr}}|\approx\frac{2(1-\lambda)}{5\lambda-1},\quad |a_{\mathrm{cr2}}|\approx 0.12. \tag{22}$$

Numerical integration of Eqs. (2) confirms this prediction. The propagation of the B component of the perturbed vectorial TU SLM (point R in Fig. 7) is plotted in Fig. 8(a). A likewise stable behavior was observed for the mode located at point S in parameter space (Fig. 7). However, a slight decrease in the secondary amplitude (transition from point R to point Q, i.e., the location of the mode changes from domain I to domain II) leads to an instability gain

$$g_{\mathrm{II}}\approx 2\left[\frac{1-\lambda}{1+\lambda}\,|a|\left(1-\frac{|a|}{|a_{\mathrm{cr1}}|}\right)\right]^{1/2},\quad \lambda<1,\quad |a|<|a_{\mathrm{cr1}}| \tag{23}$$

and the twisted unstaggered ($s=-1$, $a>0$) or twisted staggered ($s=1$, $a<0$) SLM becomes unstable [Fig. 8(b)]. Another type of unstable evolution is shown in Fig. 8(c). It

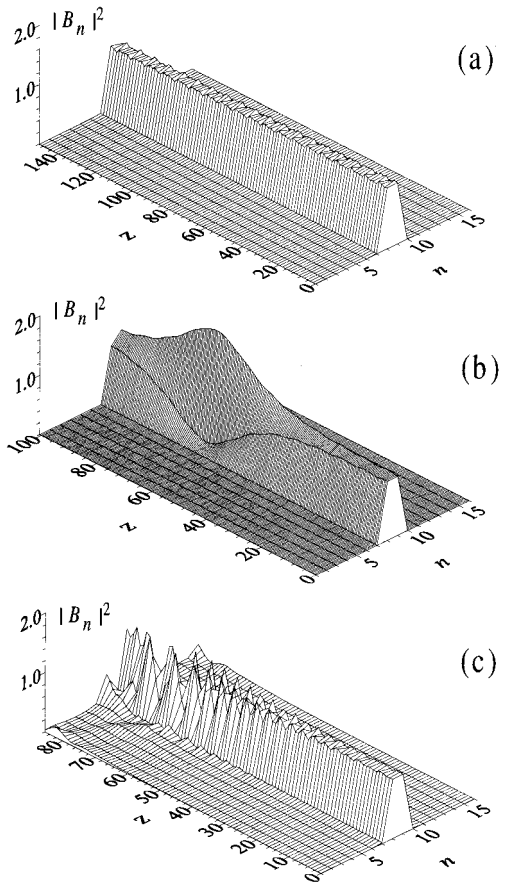

FIG. 8. Propagation of the perturbed twisted unstaggered SLM ($s=-1$). $A=B=1$, $\lambda_a=\lambda_b=\lambda$, and $c_a=c_b=c$. The B component is shown, and the A component has a similar structure. (a) $\lambda=0.9$, $c=0.12$ (point R in Fig. 7). The evolution corresponding to point S in Fig. 7 is similar. (b) $\lambda=0.9$, $c=0.07$ (point Q in Fig. 7). (c) $\lambda=1.5$ and $c=0.29$ (point T in Fig. 7).

takes place for a SLM located in region III, with a gain determined by the imaginary part of the complex eigenvalue $g_{\mathrm{III}}\approx\sqrt{(a-a_{\mathrm{cr2}})/2}$, where a_{cr2} is given by Eq. (22).

Thus one can draw the conclusion that the character of eigenvalues (real or complex) essentially determines the kind of decay of the twisted mode. It is worth mentioning that for $\lambda<1$ the *increasing* localization also results in an unstable evolution (transition to region II, see Fig. 7) which is another interesting peculiarity of twisted vectorial SLM's.

Now we leave the symmetric case ($A=B$), and proceed with a brief review of the essential features of SLM's with unequal amplitudes, where we maintain the assumption of equal coupling constants and nonlinearities. For (un)staggered modes the situation is qualitatively similar to the symmetric case: a symmetric perturbation causes no instability gain, whereas any asymmetric perturbation forces the SLM to decay. We also note that these twisted modes may also exist in other discrete systems such as Fermi-Pasta-Ulam lattices or arrays with quadratic nonlinearity [32].

As before, the twisted modes exhibit a much richer diversity of evolution scenarios. Provided that one of the peak amplitudes, say A, is fixed, an increasing ratio B/A tends to stabilize the initially unstable SLM. For instance, if the linear coupling slightly exceeds the critical value, so that the vec-

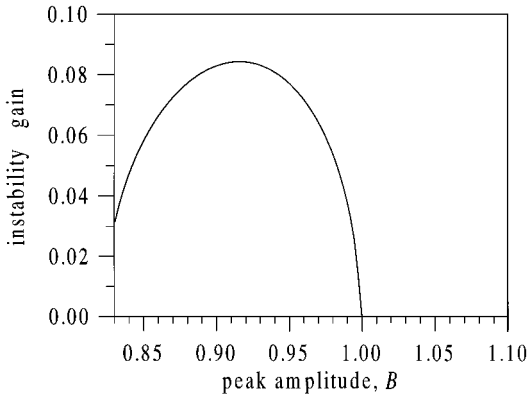

FIG. 9. Instability gain of the asymmetric twistedlike mode as a function of peak amplitude B. Parameters: $\lambda_a=\lambda_b=1.5$, $A=1.05$, $c_a=c_b=0.1$, $s_a=-0.7$, and $s_b=0.11$.

torial SLM with equal amplitudes becomes unstable, a minor increase in B (with A being constant) will stabilize the mode. Analogously, if the linear coupling is sufficiently small to guarantee a stable propagation of the symmetric mode, a decrease in B down to some critical value $B_{\rm cr}$, which is a function of c and λ, will eventually destabilize the SLM. This behavior can be easily understood recalling our previous results. The whole mode becomes unstable if the secondary excitation of *any component* exceeds the respective critical value. Thus the secondary excitation of the weaker (in the latter example B) component is responsible for the SLM's decay. Similarly to (un)staggered SLM's this dynamics implies potential applications for all-optical switching, where a slight change of the input intensity yields a strong output modulation.

If the nonlinear coefficient λ is fixed and the linear coupling c is weak, the mode is stable even for a vanishing amplitude of the second component ($B=0$). This is in agreement with the scalar limit. Some more interesting features of the SLM's dynamics were identified by numerical means. If the coupling constant $c_a=c_b=c$ corresponds to a stable situation in the scalar limit (e.g., $c=0.15$ for $\lambda=1.5$) the vectorial mode becomes unstable for a relatively large secondary excitation of the B component. However, this kind of instability occurs only in a narrow parameter region $0<B_{\rm cr1}<B<B_{\rm cr2}$. Obviously the weak second component is too poorly localized for an independent stable propagation as a scalar mode. Its trapping by the intense, *strongly localized* field A leads to a stabilization of the whole vectorial mode. If the amplitude B exceeds $B_{\rm cr1}$, but this component is still not strongly localized, the A field fails to trap, resulting in the decay of the vectorial mode. The scenario of mode disintegration is similar to that plotted in Fig. 8(c). Conversely, if the amplitude of the second component increases and exceeds $B_{\rm cr2}$, both components are strongly localized, and form a stable vectorial mode.

Another particular case, namely, that of equal self- and cross-phase modulation ($\lambda_a=\lambda_b=1$), can be treated analytically, because the eigenvalue problem factorizes into a product of four biquadratic equations. In analyzing the characteristic polynomial of Eq. (16), it can be shown that the situation completely resembles that for equal amplitudes. The SLM becomes unstable only if the secondary amplitude

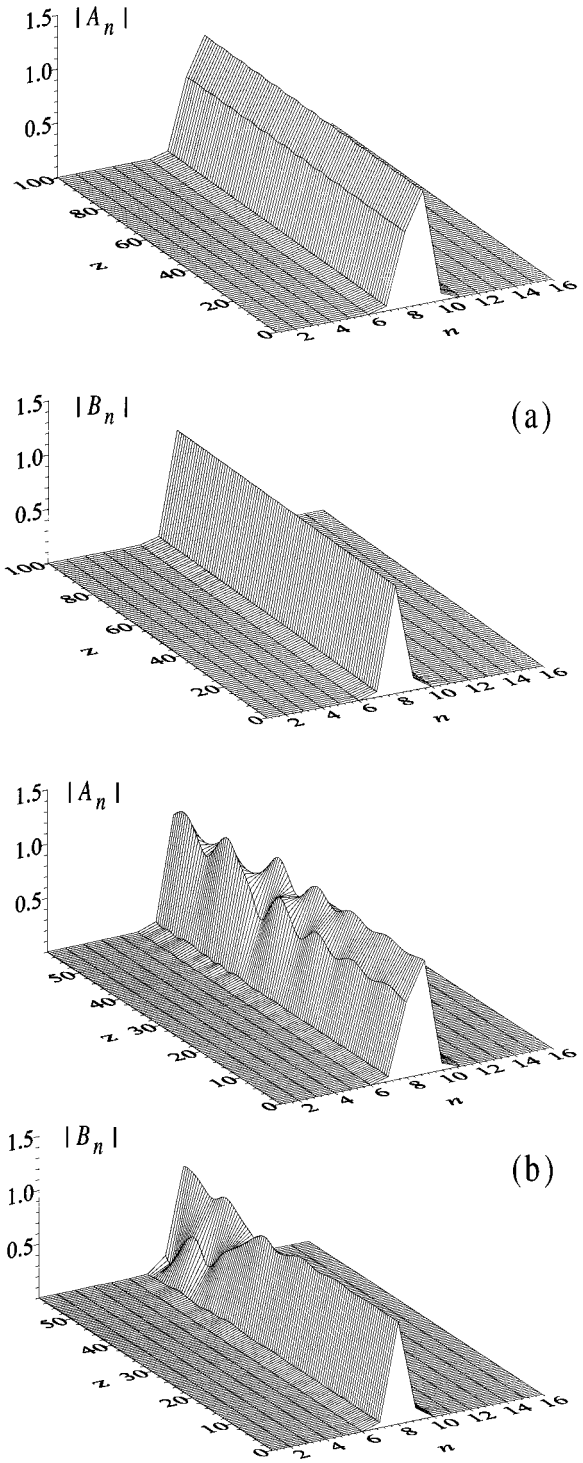

FIG. 10. Propagation of a twistedlike asymmetric vectorial SLM for the set of parameters Fig. 9. (a) $B=1$: stable. (b) $B=0.95$: unstable.

exceeds the critical value (22), which is equal for both components here. This instability is due to complex eigenvalues.

The very technique of the stability analysis can straightforwardly be extended toward odd modes. After decomposition of the perturbations into symmetric and antisymmetric ones, it is easy to realize that the system is solvable for the antisymmetric perturbations, and reveals stability against these perturbations. It remains to check the stability against

symmetric as well as perturbations of the central excitation. A straightforward calculation leads to an eigenvalue problem similar to that given by Eq. (16) for symmetrically perturbed even unstaggered SLMs. The detailed analysis yields that symmetric odd modes become unstable only beyond the strong localization limit, resulting in a spreading of the mode across the whole array. Conversely, it turns out that symmetric odd SLMs are always stable with respect to any perturbation.

Unfortunately a proper decomposition of the perturbation, that permits the simplifications used for symmetric and antisymmetric modes, fails in studying asymmetric modes. Because of the very asymmetric nature of the mode, the eigenvalue problem for the perturbations cannot be decoupled, and, even in the simplest case of the first-order calculations, a 16th-order eigenvalue problem has to be solved. In doing so we found that ''twistedlike'' asymmetric states [Fig. 3(d)] can be either stable or unstable depending on the degree of localization, whereas unstaggeredlike [Fig. 3(c)] solutions are always unstable.

As can be seen from Fig. 9, the asymmetric SLM is supposed to be stable if the peak amplitude of the B component exceeds some critical value that amounts to $B=1$ here. But, this stable propagation, shown in Fig. 10(a) can be destroyed by a slight change of the peak amplitude [Fig. 10(b)]. Note that this SLM decays more rapidly than symmetric twisted modes do. This is due to an ''intrinsic bias'' of the mode caused by the asymmetry. Hence it seems to be very promising to use this kind of mode in all-optical signal processing, because less power is needed to switch the output state. We performed numerical experiments to identify the optimum array length as well as the control signal that diminishes the peak amplitude of the B component. As can be recognized from Fig. 11, a change in the peak intensity of the B component by a few percent suffices to switch the whole power from one channel to the adjacent one completely.

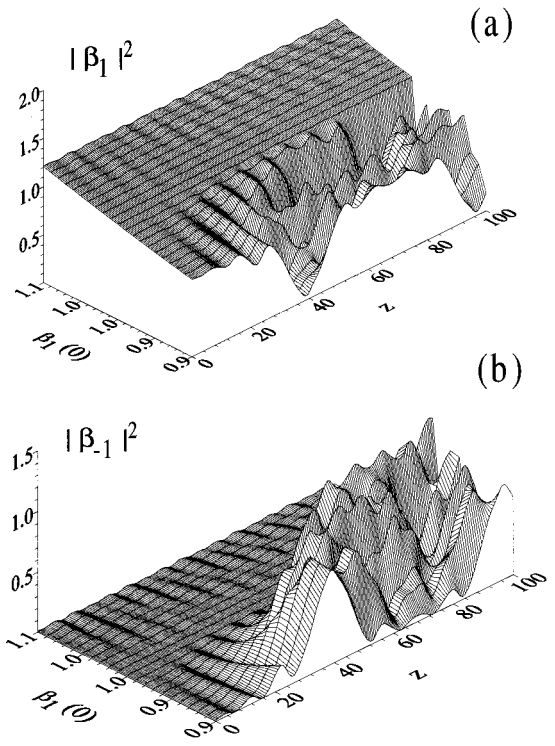

FIG. 11. All-optical switching by using asymmetric SLM's. The intensity of the B component in channels with $n=1$ (a) and $n=-1$ (b) is plotted as a function of initial amplitude in channel with $n=1$, $\beta_1(0)$, and the propagation distance.

V. CONCLUSIONS

Strongly localized, bright vectorial solutions of two coupled DNLSE's were shown to exist. In addition to conventional odd and even modes known from other discrete systems, in particular from the scalar DNLSE, interesting types of SLM's—asymmetric and shifted modes—were identified. We compared the properties of the same types of solutions in the scalar and vectorial cases. Moreover, the peculiarities of the these types of SLM's were discussed. Approximate analytic expressions for all types of SLM's were derived. Their stability was investigated by means of the linear analysis. As in the scalar scenario, odd modes appear to be stable while even (un)staggered SLM's are always unstable with respect to (anti)symmetric perturbation. Conversely, even modes with the π phase jump at the center (twisted modes) can withstand any small perturbation. The stability properties of these modes are determined by the ratio of nonlinear self- and cross modulation coefficients as well as by the degree of localization. The instability regions and the respective gain found analytically permit to derive implications for all-optical switching and logical operation.

ACKNOWLEDGMENTS

The authors gratefully acknowledge grants from the Deutsche Forschungsgemeinschaft, Bonn and the Volkswagen Stiftung, Hannover. S. D. also acknowledges partial support from NATO Linkage Grant No. 960298.

[1] A. C. Scott and L. Macneil, Phys. Lett. A **98**, 87 (1983).
[2] J. C. Eilbeck, P. S. Lomdahl, and A. C. Scott, Physica D **16**, 318 (1985).
[3] D. N. Christodoulides and R. I. Joseph, Opt. Lett. **13**, 794 (1988).
[4] Yu. S. Kivshar and D. K. Campbell, Phys. Rev. E **48**, 3077 (1993).
[5] D. Cai, A. R. Bishop, and N. Gronbech-Jensen, Phys. Rev. Lett. **72**, 591 (1994).
[6] C. Schmidt-Hattenberger, U. Trutschel, and F. Lederer, Opt. Lett. **16**, 294 (1991).
[7] C. Schmidt-Hattenberger, R. Muschall, F. Lederer, and U. Trutschel, J. Opt. Soc. Am. B **10**, 1592 (1993).
[8] M. Matsumoto, S. Katayama, and A. Hasegawa, Opt. Lett. **20**, 1758 (1995).
[9] W. Krolikowski and Yu. S. Kivshar, J. Opt. Soc. Am. B **13**, 876 (1996).
[10] A. Aceves, C. De Angelis, T. Peschel, R. Muschall, F. Lederer,

S. Trillo, and S. Wabnitz, Phys. Rev. E **53**, 1172 (1996).
[11] A. S. Dolgov, Fiz. Tverd. Tela (Leningrad) **28**, 1641 (1986) [Sov. Phys. Solid State **28**, 902 (1986)].
[12] A. J. Sievers and S. Takeno, Phys. Rev. Lett. **61**, 970 (1988).
[13] J. B. Page, Phys. Rev. B **41**, 7835 (1990).
[14] T. Dauxois and M. Peyrard, Phys. Rev. Lett. **70**, 3935 (1993).
[15] G. P. Tsironis and S. Aubry, Phys. Rev. Lett. **77**, 5225 (1996).
[16] Yu. S. Kivshar and M. Peyrard, Phys. Rev. A **46**, 3198 (1992).
[17] V. M. Burlakov, S. A. Darmanyan, and V. N. Pyrkov, Phys. Rev. B **54**, 3257 (1996).
[18] S. A. Darmanyan, I. Relke, and F. Lederer, Phys. Rev. E **55**, 7662 (1996).
[19] A. A. Aceves, G. G. Luther, C. De Angelis, A. M. Rubenchik, and S. K. Turitsyn, Phys. Rev. Lett. **75**, 73 (1995).
[20] E. W. Laedke, K. H. Spatschek, S. K. Turitsyn, and V. K. Mezentsev, Phys. Rev. E **52**, 5549 (1996).
[21] B. Denardo, B. Galvin, A. Greenfield, A. Larraza, S. Putterman, and W. Wright, Phys. Rev. Lett. **68**, 1730 (1992).
[22] P. Marquie, J. M. Bilbaut, and M. Remoissenet, Phys. Rev. E **51**, 6127 (1995).
[23] F. Kh. Abdullaev, S. A. Darmanyan, and P. K. Khabibullaev, *Optical Solitons* (Springer, New York, 1993).
[24] G. P. Agrawal, *Nonlinear Fiber Optics*, 2nd ed. (Academic, New York, 1995).
[25] S. V. Manakov, Zh. Éksp. Teor. Fiz. **65**, 505 (1974) [Sov. Phys. JETP **38**, 248 (1974)].
[26] C. R. Menyuk, IEEE J. Quantum Electron. **25**, 2674 (1989).
[27] E. W. Laedke, O. Kluth, and K. H. Spatschek, Phys. Rev. E **54**, 4299 (1996).
[28] K. W. DeLong, J. Yumoto, and N. Finlayson, Physica D **54**, 36 (1991).
[29] N. Finlayson, K. J. Blow, L. J. Bernstein, and K. W. DeLong, Phys. Rev. A **48**, 3863 (1993).
[30] K. W. Sandusky, J. B. Page, and K. E. Schmidt, Phys. Rev. B **46**, 6161 (1992).
[31] S. Darmanyan, A. Kobyakov, and F. Lederer, Zh. Éksp. Teor. Fiz. (to be published) [JETP (to be published)].
[32] S. Darmanyan, A. Kobyakov, and F. Lederer, Phys. Rev. E **57**, 2344 (1998).